

# Novel nitride – based materials for nonlinear optical signal processing applications at 1.5 $\mu\text{m}$

S. Valdueza-Felip<sup>1</sup>, F.B. Naranjo<sup>1</sup>, M. González-Herráez<sup>1</sup>, H. Fernández<sup>2</sup>, J. Solis<sup>2</sup>, S. Fernández<sup>3</sup>, F. Guillot<sup>4</sup>, E. Monroy<sup>4</sup>, J. Grandal<sup>5</sup>, M.A. Sánchez-García<sup>5</sup>.

<sup>1</sup>Grupo de Ingeniería Fotónica (GRIFO), Departamento de Electrónica, Escuela Politécnica Superior, Universidad de Alcalá. Campus Universitario, 28871 Alcalá de Henares, Madrid, Spain.

<sup>2</sup>Instituto de Óptica, C.S.I.C., Serrano 121, 28006 Madrid, Spain.

<sup>3</sup>Departamento de Investigación, Centro de Investigación y Desarrollo de la Armada, Arturo Soria 289, 28033 Madrid, Spain

<sup>4</sup>Equipe mixte CEA-CNRS-UJF « Nanophysique et Semiconducteurs », DRFMC/SP2M/PSC, CEA-Grenoble, 17 rue des Martyrs, 38054-Grenoble cedex 9, France.

<sup>5</sup>ISOM and Departamento de Ingeniería Electrónica, ETSI Telecomunicación, Universidad Politécnica de Madrid, Ciudad Universitaria, 28040 Madrid, Spain

Autor e-mail address: sirona.valdueza@depeca.uah.es

**Abstract** – We characterize the third order nonlinear optical response of the interband transition of bulk InN and the intraband transition of GaN/AlN quantum dots, both of them in the spectral region around 1.5  $\mu\text{m}$ . The results show that these materials can be very suitable for optical signal processing applications in the spectral region of wavelength-division multiplexed (WDM) transmission. Considering the temporal behavior of the nonlinear response, InN seems particularly useful in all-optical control of light speed (slow-light generation), whereas GaN/AlN quantum dots are promising for switching and wavelength conversion applications.

**Keywords** – photonic signal processing, four-wave mixing, Kerr effects, third-order susceptibility, nitride-based devices.

## I. INTRODUCTION

Semiconductor third-order nonlinear optical phenomena—like nonlinear absorption, self- and cross-phase modulation, self- and cross-gain modulation, and four-wave mixing (FWM)—have direct applications in all-optical control of data streams in fiber-optic networks [1,2]. These effects are the basis of all-optical switches and wavelength converters, to be applied in the next generation of optical networks. Recently, it has been shown that these devices can also be used for all-optical light speed control (the so-called slow and fast light phenomena) [3,4]. From the material viewpoint, the parameter responsible of these nonlinear properties is the

optical third-order susceptibility,  $\chi^{(3)}$ . Therefore, materials with large  $\chi^{(3)}$  are required for the fabrication of optically-controlled devices

There is a particular interest in the development of devices for the C band of optical fibers, around 1.5  $\mu\text{m}$ , where erbium-doped fiber amplifiers (EDFAs) are widely available. Highly nonlinear fibers and waveguides have been used for nonlinear interactions in this spectral region. However, due to the low values of their nonlinear coefficient, these solutions often require very long interaction distances (even kilometers in the case of nonlinear fibers) or very high power levels [2,3], which makes them cumbersome for a real system implementation. An interesting alternative comes through the use of semiconductors. Working in resonance conditions, the nonlinear coefficient can be extremely enhanced, requiring interaction distances of less than 1 mm for mW-level signals. Besides, the semiconductor resonance wavelength can be tuned by band-gap engineering. These properties have made semiconductor-based devices the most interesting alternative for all-optical signal processing applications [5]. In particular, an important effort on the development of InGaAs and InGaAsP-based nonlinear optical devices at 1.5  $\mu\text{m}$  has been performed in the last years.

Nonlinear interactions in nitride-based materials (specially GaN, InGaN and AlGaIn) have also been studied. Most of these studies focus on valence to conduction band (interband) optical transitions in the visible and ultraviolet regions of the electromagnetic spectrum. The recent progress in the

synthesis of InN —semiconductor with a direct bandgap around 0.65-0.7 eV (close to 1.5  $\mu\text{m}$ )— has opened new perspectives for nitride materials in the near-infrared (NIR) wavelength range. However, there is little information about the nonlinear third-order susceptibility of this material.

Another approach to extend nitride optoelectronics towards the NIR consist in using intraband transitions in quantum wells or quantum dots [6,7], profiting from the large conduction band offset ( $\sim 1.8$  eV) in the GaN/AlN system. Intraband transitions have found direct application in quantum cascade lasers [8] and quantum well infrared photodetectors (QWIPs) [9]. Rosencher *et al.* developed novel nonlinear optical materials based on intraband transitions in semiconductor quantum structures, using the second-order nonlinearities in asymmetric quantum wells [10]. The quantum confinement in semiconductor nanostructures enhances the nonlinear effects, hence enabling nonlinear interactions at low power levels. Additionally, these intraband transitions are generally faster than interband transitions, which means that they can be applied to the development of ultrafast optical devices.

In this work we have determined the third order susceptibility  $\chi^{(3)}$  at 1.5  $\mu\text{m}$  of the interband transition in bulk InN samples grown under different conditions, and showing different optical band-gap. Additionally, we have also determined the third order susceptibility at 1.5  $\mu\text{m}$  of the intraband transition in GaN/AlN quantum dots. The technique used in both cases has been the forward degenerate four-wave mixing (DFWM) technique in boxcars configuration. For the InN samples, the excitation was done at energies around the band gap (1500 nm). For the GaN/AlN quantum dots, the excitation was resonant with the *s-pz* intraband transition. By introducing a delay line in one of the arms of the experimental setup, we have also been able to determine the relaxation time of the excited carrier population grating ( $\tau_G$ ) in both kinds of samples. The results prove that these materials are suitable for optical signal processing applications in the spectral region of wavelength-division multiplexed (WDM) transmission. Considering the temporal behavior of the nonlinear response, InN seems particularly suitable for all-optical control of light speed (slow light), whereas GaN/AlN quantum dots are extremely interesting for switching and wavelength conversion applications.

Concerning slow and fast light applications, this paper will also address estimations of achievable slow-down factor in the different InN samples studied, using realistic values of pump powers and the measured nonlinear properties.

This paper is structured as follows: in Section II we described the growth conditions of the investigated samples and their linear and nonlinear optical characterization. Slow-down factor estimations for the InN samples are shown in Section III. Finally, Section IV will expound the conclusions of this study.

### A. Growth conditions

The InN samples investigated in this work were grown on Si(111) and on 10- $\mu\text{m}$ -thick non-intentionally-doped (nid) GaN-on-sapphire templates by plasma-assisted molecular beam epitaxy (PAMBE). In-situ growth monitoring was performed by Reflection High Energy Electron Diffraction (RHEED).

For InN samples grown on Si(111), the substrates were heated in the growth chamber at 800  $^\circ\text{C}$  for 30 minutes to remove the native oxide. Upon temperature decrease to 760 $^\circ\text{C}$  a clear  $7\times 7$  surface reconstruction, typical of Si(111) orientation, showed up indicating a full desorption of the native oxide. Growth on HT-AlN-buffered Si(111) was preceded by depositing a few monolayers (ML) of metallic Al at high temperature. Afterwards, the AlN buffer layer was grown at 780 $^\circ\text{C}$  at a rate as low as 200 nm/hour to minimize surface roughness according to the established optimal process [11]. Once the buffer layer is grown, the growth is stopped to decrease the temperature down to 475  $^\circ\text{C}$ , the optimal one for InN [12]. InN layers were grown under slightly indium rich conditions at a rate of 0.8  $\mu\text{m}/\text{hour}$ . A streaky  $1\times 1$  RHEED pattern observed during all the growth indicates a 2D growth mode.

In the case of the InN grown on GaN-on-sapphire templates, prior to the growth of the InN layer, a 10-nm-thick nid GaN buffer layer was deposited at 720  $^\circ\text{C}$ . InN growth was then carried out at a substrate temperature of 450  $^\circ\text{C}$ , with a N flux corresponding to a growth rate of 0.3 ML/s and with an In/N ratio of 1.2. Periodic growth interruptions under N are performed to consume the In excess and prevent the accumulation of In droplets on the surface. The growth period (InN growth time / growth interruption time) for the sample analyzed was 5 min / 1 min [13].

The GaN/AlN QD samples under study was grown by PAMBE on a 1- $\mu\text{m}$ -thick AlN-on-sapphire template. The samples consist on 20 periods of GaN QDs with 3 nm thick AlN barriers. The QD height, diameter and density was characterized by atomic force microscopy, obtaining values of  $1.2\pm 0.6$  nm,  $17\pm 3$  nm, and  $(6.4\pm 0.7)\times 10^{11}$   $\text{cm}^{-3}$ , respectively. Further details about growth conditions can be found elsewhere [14].

### B. Optical characterization conditions

Linear optical properties of InN samples in the wavelength range of 1100–2550 nm were studied at room temperature transmission measurements at normal incidence using a Perkin-Elmer Lambda 9 scanning spectrophotometer.

The nonlinear optical characterization was performed by the DFWM technique in the forward configuration (boxcars) [15] using as excitation source an optical parametric amplifier (OPA) providing 100 fs pulses, tunable in the 300–3000 nm interval, at a repetition rate of 1 kHz. In the DFWM

measurements the conjugated beam intensity  $I_c$  is plotted versus the pump intensity  $I_p$  to obtain the coefficient  $c$  of the relationship  $I_c = cI_p^3$ . The third order susceptibility of the samples,  $|\chi^{(3)}|$ , is then obtained using Eq. (1), which relates the nonlinear susceptibility of a given sample and that of a reference material with their corresponding optical parameters and conjugated signals:

$$|X_s^{(3)}| = \left( \frac{n_o^s}{n_o^r} \right) \left( \frac{L^r}{L^s} \right)^{1/2} \frac{\alpha L^s e^{\alpha L / 2}}{1 - e^{-\alpha L}} |X_r^{(3)}|, \quad (1)$$

where  $n_o$ ,  $L$ , and  $\alpha$  are the ordinary linear refractive index, the interaction length, and absorption coefficient, respectively, while superscripts  $r$  and  $s$  indicate parameters concerning the reference and the sample. The reference is a fused silica ( $\text{SiO}_2$ ) plate with  $|\chi^{(3)}| = 1.28 \times 10^{-14}$  esu and  $n_o = 1.45$  [16].

### C. Indium Nitride (InN).

Fig. 1 shows measured transmission data, for the investigated InN samples. Maximum transmittance is limited by the substrate at 0.86 and 0.53 for sapphire and silicon, respectively. Short period Fabry-Perot oscillations for the InN/GaN template sample arises from the resonant cavity formed by the structure GaN template+InN layer ( $\sim 10,6 \mu\text{m}$ ).

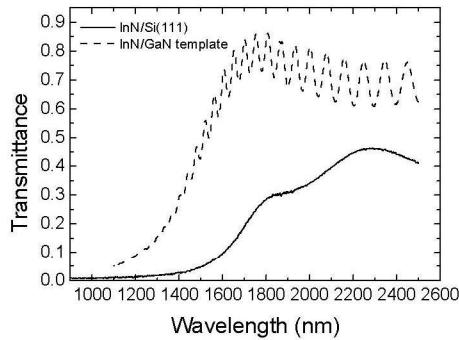


Fig. 1. Transmission spectra of the InN analyzed samples

Experimental transmission spectra were compared with theoretical calculations using a three layer model (substrate/buffer layer/InN) [17] to obtain values of thickness, ordinary refractive index  $n_o(\lambda)$ , and absorption coefficient  $\alpha(\lambda)$  of the InN layer. First order Sellmeier dispersion formulas were considered for index refraction in the transparency region [18]. Further, a sigmoidal approximation was used for  $\alpha(\lambda)$  for both samples [19]. The absorption band edge of the samples is estimated at 1550 nm (InN/GaN-template) and 1650 nm (InN/Si(111)). These values make the samples suitable for third order optical nonlinear susceptibility measurements around 1500 nm. Table I summarizes the linear optical estimations performed for 1500 nm applied to the later  $\chi^{(3)}$  calculation. Refractive index of GaN and AlN was estimated about 2.23 and 1.75 at 1500 nm,

respectively, and considering the absorption of these layers negligible.

TABLE I.

SUMMARY OF THE RESULTS OBTAINED FROM LINEAR AND NON-LINEAR OPTICAL MEASUREMENTS AT 1500 NM.

Sample	Thickness (nm)	$\alpha$ ( $\text{cm}^{-1}$ )	n	$\alpha L$	$ \chi^{(3)} $ (esu)
InN/Si(111)	950	$3 \times 10^4$	2.95	2.6	$1.9 \times 10^{-9}$
InN/GaN template	650	$4.7 \times 10^3$	2.86	0.3	$5.4 \times 10^{-10}$

Fig. 2 shows a representative plot of the conjugate beam intensity vs pump beam intensity for the InN samples.  $|\chi^{(3)}|$  values of  $(5.4 \pm 0.6) \times 10^{-10}$  and  $(1.9 \pm 0.2) \times 10^{-9}$  esu were measured at 1500 nm for InN samples grown on GaN-templates and Si(111), respectively. The obtained value increases with the linear absorption of the samples, being higher for the sample with the lowest bandgap (InN/Si(111)).

The resonant character of the involved mechanism for InN leads to values of  $|\chi^{(3)}|$  close to two orders of magnitude above the measured for GaN  $(4.4 \pm 0.4) \times 10^{-12}$  [3] and Si  $2.8 \times 10^{-11}$  esu [20] at 1500 nm. Furthermore, contribution of substrate to the measured  $|\chi^{(3)}|$  was neglected performing the DFWM experiments with a pump power below the limit to obtain a measurable nonlinear response for the substrate [13].

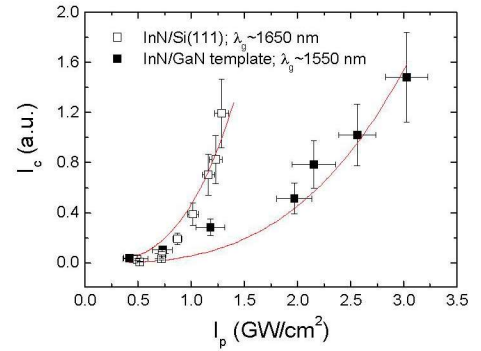


Fig. 2.  $I_c$ - $I_p$  plot of the InN samples

Fig. 3 shows the DFWM signal intensity as a function of the induced delay time for the analyzed samples. The lifetime estimated from these decay curves is of 0.8 ps for the InN sample grown on Si(111), which shows a lower bandgap energy. This lifetime is attributed to relaxation of hot carriers from higher energy states to lower energy states [21]. Lifetime estimated for InN sample grown on GaN-template, with a band gap closer to excitation wavelength is of 4.8 ps. This value is comparable to the value of 12 ps, obtained by Su *et al.* in an AsGa quantum dot based semiconductor optical amplifier, used to obtain room temperature *slow and fast light* [22]. In this case, the obtained lifetime is attributed to a non-radiative recombination mechanism, related to the defects responsible of the free carrier concentration of the layers, in the range of  $\sim 10^{19} \text{ cm}^{-3}$  [23].

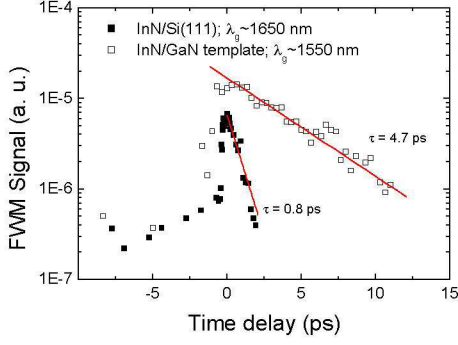


Fig. 3. DFWM signal intensity obtained as a function of delay time between one of the pumps and the others for the InN samples analyzed

#### D. GaN/AlN QDs characterization

In this section we show the experimental results for the nonlinear third order susceptibility  $\chi^{(3)}$  and the relaxation time  $\tau$  for the GaN/AlN QDs sample, using the DFWM method.

In order to measure the NIR absorption spectrum, the sample was mechanically polished to form a  $45^\circ$  multipass waveguide with five total internal reflections. The NIR absorption for  $p$ - and  $s$ -polarized light was measured at room temperature using a Fourier transform infrared (FTIR) spectrometer and a deuterated triglycine sulfate (DGTS) photodetector. For  $p$ -polarized light, we observe a Gaussian absorption peak at 0.855 eV ( $=1.4 \mu\text{m}$ ), with a full width at half maximum FWHM = 0.155 eV. The peak absorbance per pass is 1.7%. This absorption is ascribed to the transition from the  $s$ -shell ground state of the QD to the  $p_z$  excited state with one node of the envelope function along the growth axis. No absorption of  $s$ -polarized light is observed. For more details, see the reference [14].

Fig. 4 shows a representative plot of  $I_c$  vs  $I_p$  from the GaN/AlN QDs sample at the wavelength of  $1.5 \mu\text{m}$ . A clear cubic dependence between the pump intensity of the laser beam and the conjugated intensity generated by the DFWM can be observed. An ordinary refractive index of  $n_0=2.2$ , and an effective length of  $L_s=24 \text{ nm}$  were considered for the nonlinear susceptibility estimation. The measured absorbance at  $1.5 \mu\text{m}$  was 1.58 leading to an effective optical sample length of  $aL_s \sim 0.023$ . The obtained value of  $\chi^{(3)}$  is  $\sim 1.28 \times 10^{-6}$  esu, two order of magnitude higher than the obtained by Hamazaki [24], for intraband transitions in GaN/AlN quantum wells (QWs), of  $\sim 1.6 \times 10^{-8}$  esu, as expected from the dimension reduction from QW to QD.

We have also determined the lifetime  $\tau$  of the conjugated signal (associated to the dynamic grating induced at  $1.5 \mu\text{m}$ ) for sample GaN/AlN QDs by varying the delay between one of the three pumps and the others using an optical delay line. Inset of Fig. 4 shows the conjugated-signal intensity as a function of the induced delay time [25]. The measured lifetime is similar to the laser pulse width (100 fs), thus, the lifetime of the optically induced population grating in the

sample should be below this value. This result is consistent with the subpicosecond intersubband recombination times measured in GaN quantum well structures [26,27,28].

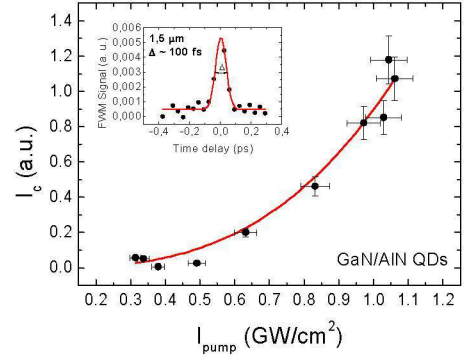


Fig. 4.  $I_c$  vs  $I_p$  plot for GaN/AlN QDs sample at  $1.5 \mu\text{m}$ . Inset shows DFWM signal intensity obtained from the sample at  $1.5 \mu\text{m}$  as a function of delay time between one of the pumps and the others

### III. SLOW-LIGHT IN INDIUM NITRIDE: ESTIMATION OF SLOW-DOWN FACTORS

The nonlinear absorption coefficient was obtained for the InN samples using the following equation [28]:

$$\alpha_2 = \frac{3\nu_0 \text{Im}(\chi^{(3)})}{2\epsilon_0 n_0^2 c^2} \quad (2)$$

where,  $\nu_0$  and  $n_0$  are the resonance frequency and the linear refractive index at this frequency, respectively. The imaginary part of  $\chi^{(3)}$  was considered to be of the same order of magnitude of  $\chi^{(3)}$ . Values of  $\alpha_2$  of 79 cm/GW and 24 cm/GW were obtained for InN/Si(111) and InN/GaN template, respectively.

The change in refractive index and absorption from  $\alpha_2$  and the measured recombination time [29] was calculated considering a Lorentzian-type line shape. This line shape leads to a phase-change of the wave travelling across the sample of [30]:

$$\phi = L_{\text{eff}} \frac{\alpha_2 I}{2} \frac{\left( \nu - \nu_0 / (\Delta\nu/2) \right)}{1 + \left( \nu - \nu_0 / (\Delta\nu/2) \right)^2} \quad (3)$$

where  $\Delta\nu$  is the Full Width at Half Maximum (FWHM) bandwidth. This bandwidth was calculated as the inverse of the measured population grating lifetime, obtaining a value of 398 GHz and 66 GHz, for InN/Si(111) and InN/GaN template, respectively, while  $\nu_0$  is the resonance frequency, of 200 THz.  $L_{\text{eff}}$  is calculated using  $L_{\text{eff}} = (1 - e^{-\alpha}) \cdot \alpha^{-1}$  and accounts for the effective length of the sample. This factor takes into account the linear absorption of the sample. The slow-down factor of the sample, is then obtained through

$S = \left( \frac{c}{2\pi \cdot z} \right) \frac{d\phi}{dv}$  leading to a maximum values of 0,5 and 3,6 for InN/Si(111) and InN/GaN template, respectively, for a typical pump intensity of 3 GW/cm<sup>2</sup> and a sample thickness of 2 μm. Sample with lower bandgap energy (InN/Si(111)) shows a lower slow-down factor, as expected from its higher linear absorption at the analyzed wavelength of 1500 nm (see Table I). Fig. 5a and 5b show respectively the absorption change and slow-down factor calculated considering the above described conditions. Absorption saturation has been observed in InN thick layers [23], pointing out a negative sign of  $\alpha_2$  in this material, as it is shown in fig. 5a.

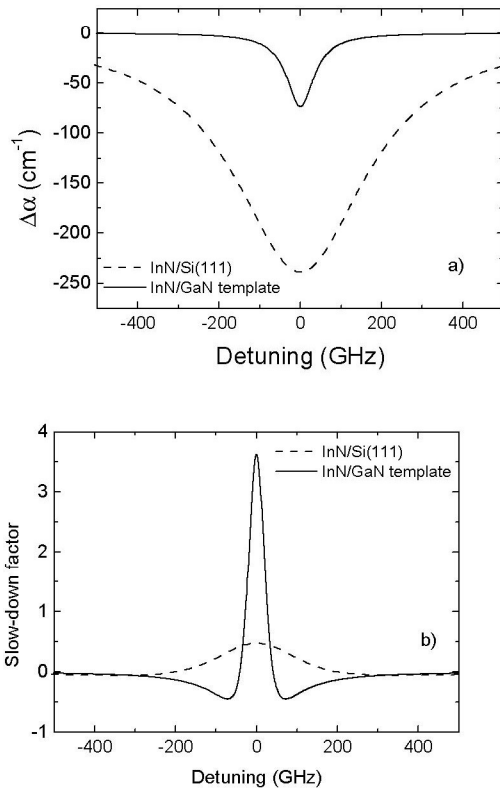


Fig. 5. Calculated nonlinear absorption (a) and slow-down factor (b) of analyzed InN samples at 1500 nm as a function of detuning, considering excitation pump power of 3 GW/cm<sup>2</sup>

Simulations performed show that this slow-down factor could be increased three or more orders of magnitude by using quantum well structures since in these structures the values of  $\chi^{(3)}$  and  $\tau$  are two or three orders of magnitude larger than in the bulk material [31,32]. This would open the possibility of using InN-based heterostructures for slow-light applications.

#### IV. CONCLUSIONS

In this work we have measured the third order susceptibility,  $\chi^{(3)}$ , of InN films grown by PAMBE with different optical bandgap energy, by using DFWM technique at 1.5 μm.  $\chi^{(3)}$  and population grating life time,  $\tau$  of  $1.9 \times 10^{-9}$

esu and 0.8 ps, respectively, were measured for samples with optical bandgap corresponding to 1650 nm, grown on Si(111). At the same time,  $\chi^{(3)}$  and  $\tau$  of  $0.54 \times 10^{-9}$  esu and 4.7 ps, respectively, were measured for samples grown on GaN template, which shows an optical bandgap of 1550 nm. Linear absorption at the analyzed wavelength together with the relaxation mechanism involved in the nonlinear response are responsible of the different values of  $\chi^{(3)}$  and population grating life time obtained depending on the optical band gap of the samples. A maximum slow-down factor of 3.6 was obtained for InN sample with the optical band gap closer to the excitation wavelength for a pump intensity of 3 GW/cm<sup>2</sup>, and taking into account the linear absorption of the layer. Simulations performed show that this slow-down factor could be increased three or more orders of magnitude by using quantum well structures since in these structures the values of  $\chi^{(3)}$  and  $\tau$  are two or three orders of magnitude larger than in the bulk material [31,32]. This would open the possibility of using InN-based heterostructures for slow-light applications.

The results on GaN/AlN QDs show that these structures are promising for switching and wavelength conversion applications, for the spectral region of WDM.

#### ACKNOWLEDGMENT

Partial financial support was provided by Spanish government projects TEC2006-09990-C02-02/TCM and TEC2005-00074/MIC, and by Comunidad de Madrid, Project S-0505/AMB-0374.

#### REFERENCES

- [1] R. W. Boyd, "Nonlinear optics" Academic Press, San Diego (2003).
- [2] S. Radic and C. J. McKinstrie, "Optical amplification and signal processing in highly nonlinear optical fiber", IEICE Trans. Electron. E88-C, 859 (2005).
- [3] R. W. Boyd and D. J., "'Slow" and "fast" light", Gauthier Progress in Optics 43, 497 (2002).
- [4] M. Gonzalez-Herraez, K. Y. Song and L. Thevenaz, "Optically controlled slow and fast light in optical fibers using stimulated Brillouin scattering", Appl. Phys. Lett. 87 08113 (2005).
- [5] D. N. Maywar and G. P., "Robust optical control of an optical-amplifier-based flip-flop", Agrawal Opt. Express6, 75 (2000).
- [6] M. Tchernycheva, L. Nevou, L. Doyennette, F. H. Julien, E. Warde, F. Guillot, E. Monroy, E. Bellet-Amalric, T. Remmele, and M. Albrecht, "Systematic experimental and theoretical investigation of intersubband absorption in GaN/AlN quantum wells", Phys. Rev. B 73, 125347 (2006).
- [7] F. Guillot, E. Bellet-Amalric, E. Monroy, M. Tchernycheva, L. Nevou, L. Doyennette, F. H. Julien, L. S. Dang, T. Remmele, M. Albrecht, T. Shibata, and M. Tanaka, "Si-doped GaN/AlN quantum dot superlattices for optoelectronics at telecommunication wavelengths", J. Appl. Phys. 100, 044326 (2006).
- [8] J. Faist, F. Capasso, D. L. Sivco, C. Sirtori, A. L. Hutchinson, and A. Y. Cho, "Quantum cascade laser", Science 264, 553 (1994).
- [9] B. F. Levine, "Quantum well infrared photodetectors", J. Appl. Phys. 74, R1 (1993).
- [10] E. Rosencher and Ph. Bois, "Model system for optical nonlinearities: asymmetric quantum wells", Phys. Rev. B, vol. 44, no. 20, pp. 11315 – 11327 (1991).
- [11] E. Calleja, M.A. Sánchez-García, F.J. Sánchez, F. Calle, F.B. Naranjo, E. Muñoz, S.I. Molina, A.M. Sánchez, F.J. Pacheco and R. García, "Growth of III-nitrides on Si(111) by molecular beam epitaxy Doping, optical, and electrical properties", J. Crys. Growth 201/202, 296 (1999).

- [12] J. Grandal and M.A. Sánchez-García, "InN layers grown on silicon substrates: effect of substrate temperature and buffer layers", *J. Cryst. Growth*, 278, 373 (2005).
- [13] F.B. Naranjo, M. González-Herráez, H. Fernández, J. Solís, E. Monroy, "Third order nonlinear susceptibility of InN at near band-gap wavelengths", *Appl. Phys. Lett.* 90, 091903 (2007).
- [14] F. Guillot, E. Bellet-Amalric, E. Monroy, M. Tchernycheva, L. Nevou, L. Doyennette, F.H. Julien, L. S. Dang, T. Remmele, M. Albrecht, T. Shibata, and M. Tanaka, "Si-doped GaN/AlN quantum dot superlattices for optoelectronics at telecommunication wavelengths", *J. Appl. Phys.* 100, 044326 (2006).
- [15] R.L. Sutherland, "Handbook of nonlinear optics" Marcel Dekker, Inc., New York (1996).
- [16] P. Palinginis, F. Sedgwick, S. Crankshaw, M. Moewe, and C. J. Chang-Hasnain, "Room temperature slow light in a quantum-well waveguide via coherent population oscillation", *Opt. Express* 13, 9909 (2005).
- [17] M.J. Bergman, Ü. Özgür, H.C. Casey, J.F. Muth, Y.C. Chang, R.M. Kolbas, R.A. Rao, C.B. Eom, and M. Schurman, "Linear optical properties of a heavily Mg-doped AlGaIn epitaxial layer", *Appl. Phys. Lett.* 74, 3188 (1999).
- [18] N. Antoine-Vincent, F. Natali, M. Mihailovic, A. Vasson, J. Leymarie, P. Disseix, D. Byrne, F. Semond, and J. Massies, "Determination of the refractive indices of AlN, GaN, and AlGaIn grown on Si(111) substrates" *J. Appl. Phys.* 93, 5222 (2003).
- [19] F.B. Naranjo, M.A. Sánchez-García, F. Calle, E. Calleja, B. Jenichen, and K.H. Ploog, "Strong localization in InGaIn layers with high indium content grown by molecular beam epitaxy" *Appl. Phys. Lett.* 80, 231 (2002).
- [20] D. Dimitropoulos, V. Raghunathan, R. Claps, and B. Jalali, "Phase-matching and nonlinear optical processes in silicon waveguides", *Opt. Exp.* 12, 149 (2004).
- [21] F. Chen, A. N. Cartwright, H. Lu, W. J. Schaff, "Ultrafast carrier dynamics in InN epilayers" *J. Cryst. Growth* 269, 10 (2004).
- [22] H. Su, and S.L. Chuang, "Room temperature slow and fast light in quantum-dot semiconductor optical amplifiers" *Appl. Phys. Lett.* 88, 061102 (2006).
- [23] F. Chen, A. N. Cartwright, H. Lu, J. Schaff, "Time-resolved spectroscopy of recombination and relaxation dynamics in InN" *Appl. Phys. Lett.* 83, 4984 (2003).
- [24] R. Rapaport, G. Chen, O. Mitrofanov, C. Gmachl, N. M. Ng, and S. N. G. Chu, "Resonant optical nonlinearities from intersubband transitions in GaN/AlN quantum wells", *Appl. Phys. Lett.* 83, 263 (2003).
- [25] S. Adachi, Y. Takagi, J. Takeda, and K.A. Nelson, "Optical sampling four-wave-mixing experiment for exciton relaxation processes" *Optics Communications* 174, 291 (2000).
- [26] N. Iizuka, K. Kaneko, N. Suzuki, "Near-infrared intersubband absorption in GaN/AlN quantum wells grown by molecular beam epitaxy", *Appl. Phys. Lett.* 81, 1803 (2002).
- [27] N. Iizuka, K. Kaneko, N. Suzuki, "Near-infrared intersubband absorption in GaN/AlN quantum wells grown by molecular beam epitaxy", *Appl. Phys. Lett.* 81, 1803 (2002).
- [28] J. D. He, C. Gmachl, H. M. Ng, and A. Y. Cho, "Comparative study of ultrafast intersubband electron scattering times at similar to 1.55  $\mu$ m wavelength in GaN/AlGaIn heterostructures", *Appl. Phys. Lett.* 81, 1803 (2002).
- [29] M. Sheik-Bahae, M. P. Hasselbeck, "Third Order Optical nonlinearities" *OSA Handbook of Optics, Vol IV. Chapter 12.* (2000).
- [30] L. Thévenaz, K. Y. Song, M. González-Herráez, "Time biasing due to the slow-light effect in distributed fiber-optic Brillouin sensors" *Opt. Lett.* 31, 715 (2006).
- [31] K. D. Choquette, L. McCaughan, D.K. Misemer, "Third-order optical susceptibility in short-period GaAs doping superlattices", *J. Appl. Phys.* 66, 4387 (1989).
- [32] A. Sasaki, K. Nishizuka, T. Wang, S. Sakai, A. Kaneta, Y. Kawakami, Sg. Fujita, "Radiative carrier recombination dependent on temperature and well width of InGaIn/GaN single quantum well", *Solid Stat. Comm.* 129, 31 (2004).